Journal of Experimental Botany, Vol. 62, No. 15, pp. 5367–5384, 2011
doi:10.1093/jxb/err197 Advance Access publication 12 August, 2011
This paper is available online free of all access charges (see http://jxb.oxfordjournals.org/open_access.html for further details)

Journal of Experimental Botany
www.jxb.oxfordjournals.org

RESEARCH PAPER

Label-free shotgun proteomics and metabolite analysis reveal a significant metabolic shift during citrus fruit development

Ehud Katz[1], Kyung Hwan Boo[1], Ho Youn Kim[1], Richard A. Eigenheer[2], Brett S. Phinney[2], Vladimir Shulaev[3], Florence Negre-Zakharov[1], Avi Sadka[4] and Eduardo Blumwald[1,*]

[1] Department of Plant Sciences, University of California, Davis, CA 95616, USA
[2] Genome Center, Proteomics Core Facility, University of California, Davis, CA 95616, USA
[3] Department of Biological Sciences, University of North Texas, TX 76203-5017, USA
[4] Department of Fruit Tree Species, ARO, The Volcani Center, 50250 Bet Dagan, Israel

* To whom correspondence should be addressed. E-mail: eblumwald@ucdavis.edu

Received 8 April 2011; Revised 17 May 2011; Accepted 20 May 2011

Abstract

Label-free LC-MS/MS-based shot-gun proteomics was used to quantify the differential protein synthesis and metabolite profiling in order to assess metabolic changes during the development of citrus fruits. Our results suggested the occurrence of a metabolic change during citrus fruit maturation, where the organic acid and amino acid accumulation seen during the early stages of development shifted into sugar synthesis during the later stage of citrus fruit development. The expression of invertases remained unchanged, while an invertase inhibitor was up-regulated towards maturation. The increased expression of sucrose-phosphate synthase and sucrose-6-phosphate phosphatase and the rapid sugar accumulation suggest that sucrose is also being synthesized in citrus juice sac cells during the later stage of fruit development.

Key words: Citrus, fruit development, juice sac cells, LC-MS/MS, proteomics.

Introduction

Citrus is one of the most important and widely grown commodity fruit crops (Talon and Gmitter, 2008). Citrus has a non-climacteric fruit maturation behaviour and a unique anatomical fruit structure (Spiegel-Roy and Goldschmidt, 1996). The fruit contains two peel tissues, flavedo and albedo. The flavedo accumulates pigments and compounds which contribute to the fruit aroma, while the albedo comprises spongy cells rich in pectin. During the early stages of fruit development the albedo occupies most of the fruit volume and it becomes gradually thinner during fruit development as the juice cells in the pulp grow (Spiegel-Roy and Goldschmidt, 1996). Growth and development of the citrus fruit can be divided into three major stages (Bain, 1958; Katz *et al.*, 2004). Stage I starts immediately after fruit set and is characterized by extensive cell division. During the transition to stage II, cell division ceases in all fruit tissues except the outermost flavedo layers and the tips of the juice sacs. During this stage, citrus fruit grows through cell expansion. Juice sac cell enlargement is mostly driven by the expansion of the vacuole, which occupies most of the cell volume. Stage III is the fruit maturation and ripening stage when fruit growth slows down and the pulp reaches its final size. Citrus fruit development is characterized by changes in primary and secondary metabolite content, with sugars and citric acid being the major components of the juice sac cells. Sucrose is translocated to the fruits from the leaves throughout fruit development, and constitutes about 50% of the total soluble sugars. The anatomy of the citrus fruit, where the juice sacs are disconnected from the vascular bundles present in the albedo, suggest apoplastic sucrose downloading (Lowell *et al.*, 1989; Tomlinson *et al.*, 1991; Koch, 2004). Sucrose can then be hydrolysed by cytosolic invertases or stored in

the acidic vacuoles and hydrolysed by vacuolar acidic invertases (Echeverria, 1992; Echeverria and Burns, 1990). Accumulation of citric acid in the vacuole of the juice sac cells is correlated with vacuole acidification mediated by the proton pumping activity of the tonoplastic H^+-ATPase. Citrate begins to accumulate during the second phase of fruit development. The accumulation continues for a few weeks, reaching a peak when the fruit volume is about 50% of its final value and then acid declines gradually as the fruit matures (Shimada *et al.*, 2006). Citrate decline during the second half of fruit development is associated with the activity of CsCit1, a H^+/citrate symporter (Shimada *et al.*, 2006). It has been suggested that some of the citrate is targeted for amino acid biosynthesis generally induced during the second half of fruit development (Sadka *et al.*, 2002). Indeed, there is an increase in some amino acid metabolizing genes, including those of the GABA shunt, and their corresponding enzymes during the citrate decline stage (Cercos *et al.*, 2006; Katz, *et al.*, 2007).

In the last few years, studies using transcriptome analysis and metabolite profiling demonstrated a tight regulation of fruit metabolism during fruit maturation (Carrari *et al.*, 2006; Mounet *et al.*, 2009; Zanor *et al.*, 2009). However, comparison of mRNA expression levels, proteins amounts, and enzymatic activities have revealed low correlations between metabolome and transcriptome, indicating that transcriptome analysis was not sufficient to understand protein dynamics or biochemical regulation (Gygi *et al.*, 1999; Gibon *et al.*, 2006; Wienkoop *et al.*, 2008). A more direct correlation is expected for proteins and metabolites (Wienkoop *et al.*, 2008) and, therefore, quantitative mass spectrometric (MS) proteomics and metabolomics are becoming attractive approaches. Quantitative proteomics has been used for the quantification of complex biological samples (Bantscheff *et al.*, 2007; America and Cordewener, 2008; Schulze and Usadel, 2010). Previously, LC-MS/MS was used to identify the proteome of various cellular fractions of the juice sac cell (Katz *et al.*, 2007). More recently, a label-free differential quantitative mass spectrometry method was developed to follow protein changes in citrus juice sac cells. Two alternative methods, differential mass-spectrometry (dMS) and spectral counting (SC) were used to analyse the protein changes occurring during the earlier and late stages of fruit development (Katz *et al.*, 2010). Along with the generation of a novel bioinformatics tool, iCitrus, the above method enabled the identification of approximately 1500 citrus proteins expressed in fruit juice sac cells and the quantification of changes in their expression during fruit development.

In this study, label-free LC-MS/MS-based shot-gun proteomic and metabolomic approaches were utilized to investigate citrus fruit development. These tools were used to identify and evaluate changes occurring in the metabolic pathways of juice sac cells which affect citrus fruit development and quality. Integration of proteomic and metabolomic analyses created a more comprehensive overview of changes in protein expression and metabolite composition of primary metabolism during citrus fruit development and maturation.

Materials and methods

Plant material and protein isolation

Orange Navel (*Citrus sinensis* cv. Washington) fruits at three different developmental stages, early stage II, stage II, and stage III (35, 55, and 80 mm in fruit diameter, respectively) (Katz *et al.*, 2004) were obtained from the Lindcove Research Center, University of California, Exeter, CA. Juice sacs were collected from at least 20 fruits and pooled at each stage. Two independent biological repetitions from two consecutive years were used. Soluble and membrane-bound proteins were isolated as described by (Katz *et al.* 2007, 2010).

Mass spectrometry and data analysis

Digested peptides were separated by reverse-phase chromatography and the separated peptides were analysed in a Thermo-Scientific LTQ-FT Ultra mass-spectrometer (San Jose, CA) as described previously (Katz *et al.*, 2010). Five technical replications of each pooled sample (older versus younger fruit) were run with blanks (washes) between each sample run. Tandem mass spectra were extracted with Xcalibur version 2.0.7. All MS/MS samples were analysed using SEQUEST (Protein Discoverer 1.1; Thermo-Scientific, San Jose, CA). SEQUEST was set up to search a FASTA file of the iCitrus Protein Database (Katz *et al.*, 2010), assuming the digestion enzyme trypsin. SEQUEST parameters were as before (Katz *et al.*, 2010). The filtering criteria consisted of Cross-correlation (xcorr) values larger than 1.5 for single-charged ions, 2.2 for double-charged ions, and 3.3 for triple-charged ions, for both half or fully tryptic peptides. This resulted in a false discovery rate of less than 5% using a decoy database search strategy.

For differential expression mass spectrometry (dMS), samples were analysed using a Thermo Scientific LTQ-FT mass-spectrometer and a Michrom-Paradigm HPLC. Peptides were separated according to Katz *et al.* (2010) and analysed using the label-free differential expression package SIEVE 1.3. (Thermo Scientific, San Jose Ca). Search results were filtered for a false discovery rate of 5% also employing a decoy search strategy utilizing a reverse database (Elias *et al.*, 2005; Kall *et al.*, 2008)

For spectral counting, all MS/MS samples were analysed using X! Tandem (www.thegpm.org; version TORNADO (2008.02.01.2)). X! Tandem was set up to search the 62,415 entries of iCitrus (Katz *et al.*, 2010) assuming the digestion enzyme trypsin. Scaffold 2.06.00 (Proteome Software Inc., Portland, OR) was used to validate MS/MS-based peptide and protein identifications. Peptide identifications were accepted if they could be established at greater than 80% probability as specified by the Peptide Prophet algorithm (Keller *et al.*, 2002). Protein identifications were accepted if they could be established at greater than 95% probability and contained at least two identified peptides. Protein probabilities were assigned by the Protein Prophet algorithm (Nesvizhskii *et al.*, 2003). Proteins that contained similar peptides and could not be differentiated based on MS/MS analysis alone were grouped to satisfy the principles of parsimony. Unweighted spectral counts for the identified proteins obtained from the samples corresponding to two consecutive growth seasons were exported from Scaffold and analysed using QSpec (Choi *et al.*, 2008) for significance analysis. Proteins were considered significantly different across sample conditions if QSpec reported a Bayes factor of >10. This corresponded to a false discovery rate (FDR) of approximately 5% (Katz *et al.*, 2010).

Because of the use of different software packages and different FDR calculations, caution should be used when comparing the label-free data with the spectral counting.

Proteomics data set

The data associated with this manuscript may be downloaded from ProteomeCommons.org Tranche using the following hash:

Cf3G8KatEeCbDv2kV1Gnw4njaSYARJgmtyzYl+5764Gsbb/M3LX+/oo1zcHnHK1Gs0ukuBM5Rk+Q1t5hpia109pVPXkAA-AAAAAAoLg==

The hash may be used to prove exactly what files were published as part of this manuscript's data set, and the hash may also be used to check that the data have not changed since publication.

Extraction and derivatization of polar metabolites

Citrus juice sacs were immediately frozen after removal in liquid nitrogen and stored at –80 °C until further analysis. For extraction of polar metabolites, samples were lyophilized and ground, and the powder (10 mg) was mixed with 250 µl of 75% ice-cold methanol and two stainless steel balls (2.3 mm). Metabolites were extracted twice using a Retsch Mixer Mill (30 s at 30 cycles s^{-1}) (Retsch Inc., Newtown, PA) and placed on dry ice for 15 min. A 250 µl aliquot of 25% methanol with an internal standard (12 µg ml^{-1} ribitol in water) was added to each sample and subjected to two more treatment cycles in the mixer mill. The mixture was vortexed, and then centrifuged at 13 000 rpm for 20 min. The liquid fraction was carefully transferred to a new vial and 200 µl of chloroform were added. The mixture was briefly vortexed and centrifuged at 2600 *g* for 20 min. The upper polar fraction was carefully aliquoted into 1.5 ml vials and dried *in vacuo*. Metabolites were methoximated with 80 µl of methoxylamine hydrochloride in pyridine (20 mg·ml^{-1}) for 90 min at 45 °C. Metabolites were then trimethylsilylated with 80 µl of MSTFA+1%TMCS (*N*-methyl-*N*-trimethylsilyltrifluoroacetamide and trimethylchlorosilane, Pierce, Rockford, IL) for 30 min at 37 °C. After derivatization, a 1 µl aliquot was analysed by GC-MS (Roessner *et al.*, 2000). Standard chemicals were derivatized with methoxyamine hydrochloride solution in pyridine and MSTFA as described above.

GC/MS analysis

Samples were injected into a hot (230 °C) injector with a split ratio of 25:1. Compounds were separated on a non-polar Alltech AT-5ms column (25 m+5 m guard×0.25 mm ID×0.25 µm film thickness) using helium at 1 ml min^{-1} as the carrier gas. The oven programme was 70 °C for 5 min, 5 °C min^{-1} ramp to 310 °C, 1 min hold, and 2 min equilibration (Trace GC, Thermo Electron Corp.). The interface and ion source temperatures were 250 °C and 200 °C, respectively. Analytes were detected using a dual-stage single quadrupole mass selective detector (Trace DSQ, Thermo Electron Corp.). Mass spectra were recorded at 2 scans s^{-1} with a 50–600 *m/z* scanning range.

Metabolites were identified using spectral matching and retention indexes from custom in-lab libraries in AMDIS (automated mass spectral deconvolution and identification system, NIST, Gaithersburg, MD). Metabolite peak areas were integrated using the ICIS algorithm in Xcalibur v2.0. Statistical analysis of peak area and the calculation of targeted metabolites with external calibration curves was done using the SAS system v9.1 (SAS Institute, Cary, NC).

MAPMAN analysis

MapMan (http://mapman.gabipd.org/web/guest) BINs, currently used for *Arabidopsis* classification (Thimm *et al.*, 2004; Usadel *et al.*, 2005), were adopted for citrus using iCitrus (Katz *et al.*, 2010). For visualization, the *Arabidopsis* homologues of citrus proteins were loaded into MapMan, which displays individual genes mapped on their pathway as false colour-coded rectangles. To facilitate comparison of the different colours, a legend explaining the changes is displayed by MapMan, which associates the colour representation with the log fold changes in protein expression.

RNA extraction

RNA was extracted from frozen juice sac tissues of Navel oranges, first by grinding 0.5 g of tissue in liquid nitrogen into a fine powder. The ground tissue was mixed with cold extraction buffer (TRIS/HCl pH 8 200 mM, EDTA 25 mM, NaCl 75 mM, SDS 1%, and β-mercaptoethanol 1 M). The same volume of phenol/chloroform/iodoacetamide (25/24/1, by vol.) was then added, mixed, and centrifuged at 10 000 *g* for 15 min. The supernatant was collected and an equal volume of pure ethanol was added, mixed by inversion and incubated at –20 °C for 15 min. This mixture was then centrifuged at 10 000 *g* for 10 min at 4 °C. The supernatant was collected and nucleic acids were precipitated by first adding 1/10 (v/v) of 3 M Na-acetate (pH 5.2) and 2 vols of 100% ethanol. After storing the samples at –20 °C for 20 min, they were then centrifuged at 12 000 *g* for 15 min. The pellet was retained and re-suspended in sterile water. RNA was selectively precipitated overnight at 4 °C by adding LiCl to a final concentration of 2 M, then the samples were centrifuged at 12 000 *g* for 15 min at 4 °C and then washed with 70% ethanol, after which samples were re-suspended in 50 µl of sterile water.

Quantitative PCR analysis

RNA was extracted from juice sac cells at early stage II, stage II, and stage III with three biological replicates. First-strand cDNA was synthesized from 1 µg of total RNA with the QuantiTect Reverse Transcription Kit (Qiagen, Valencia, CA). Primer3 software (ver. 0.4.0; http://frodo.wi.mit.edu/primer3/) was used for primer design. Quantitative PCR was performed on the StepOnePlus™ (Applied Biosystems, Foster City, CA, USA), using SYBR® Green. A total reaction volume of 15 µl was used. The reaction mix included 2 µl template, 0.3 µl of reverse primer, 0.3 µl of forward primer, 7.5 µl SYBR Green Master Mix, and 4.9 µl RNA-free water. A qPCR assay was performed using the following conditions: 95 °C for 10 min followed by 40 cycles of 95 °C for 30 s and 60 °C for 30 s. The $2^{-\Delta\Delta CT}$ method (Livak and Schmittgen, 2001) was used to normalize and calibrate transcript values relative to the endogenous citrus 18S ribosomal protein, whose expression did not change across citrus fruit developmental stages. Primer sequences are described in Supplementary Table S3 at *JXB* online.

Enzymatic assays

Protein extraction

Frozen juice sac samples were ground in liquid nitrogen with 1 mg of insoluble PVPP (polyvinyl polypyrrolidone) to remove polyphenols harmful to proteomics analysis. Total protein was extracted with 4 vols (w/v) of extraction buffer containing 50 mM HEPES-KOH pH 7.5, 10 mM $MgCl_2$, 1 mM EDTA, 2 mM DTT, 1 mM PMSF, 0.1% (v/v) Triton X-100, and 10% glycerol. The extract was centrifuged at 4 °C and 12 000 *g* for 10 min. The supernatant was desalted with a Sephadex-G25 gel column pre-equilibrated with ice-cold extraction buffer containing no Triton X-100 nor PVPP. The protein fraction was collected in pre-chilled tubes and used for enzymatic assays. Protein concentration was determined according to Bradford (1976) using BSA as a standard.

Sucrose-phosphate synthase (SPS) assay

SPS activity was assayed by quantifying the fructosyl moiety of sucrose using the anthrone test (Baxter *et al.*,

2003). Samples were incubated for 30 min at 25 °C in 200 µl of buffer containing 50 mM HEPES-KOH pH 7.5, 20 mM KCl, 4 mM $MgCl_2$, 4 mM UDP-Glc, 2 mM Fru-6-P (in a 1:4 ratio with Glc-6-P), and 5 mM KH_2PO_4. The reaction was terminated by incubation at 95 °C for 5 min and samples were centrifuged at 4 °C and 12 000 *g* for 5 min. To neutralize unreacted hexose phosphate, 100 µl of the supernatant was mixed with 100 µl of 5 M KOH and incubated at 95 °C for 10 min. Samples were mixed with 4 vols of 0.14% (w/v) anthrone reagent in 14.6 M H_2SO_4 and incubated at 95 °C for 10 min. Absorbance was measured at 620 nm. Blank samples containing boiled protein and reaction buffer without hexose phosphates were prepared by the same procedure. The absolute amount of sucrose-6-P created by the reaction was calculated using a sucrose standard curve.

Sucrose-phosphate phosphatase assay (SPP)

SPP activity was assayed by quantifying the released orthophosphate from Suc-6-P (Lunn *et al.*, 2000). Protein extract was mixed with 150 µl of buffer containing 25 mM HEPES-KOH pH 7.0, 8 mM $MgCl_2$, and 1.25 mM Suc-6-P, and incubated for 30 min at 30 °C. The reaction was stopped by adding 30 µl of 2 M trichloroacetic acid. Orthophosphate in the sample was measured using an ascorbic acid–ammonium molybdate reagent (Harwood *et al.*, 1969).

Statistical analysis

The JMP® 8.0 statistical package (SAS Institute, Cary, NC) was used for all statistical analyses. An agglomerative hierarchical procedure with an incremental sum of squares grouping strategy, known as Ward's method (Ward, 1963), was used for the purpose of classification the metabolites into similar expression groups.

Results

Changes in proteins associated with sugar metabolism and homeostasis during citrus fruit development

An extensive comparative proteomics study was conducted in order to identify protein changes occurring during citrus fruit growth and development. Samples were collected from three developmental stages; early stage II, stage II, and stage III (35, 55, and 80 mm fruit diameter, respectively). For proteomics analysis, two biological repetitions from two consecutive years were collected from at least 20 pooled fruits for each stage (Katz *et al.*, 2010). For gene expression, enzyme activities, and metabolome analysis, three biological repetitions of three consecutive years were analysed. For better identification of differentially expressed proteins during fruit development and to decrease sample complexity, the juice sac cells were fractionated into soluble and membrane-bound proteins (Katz *et al.*, 2010). Changes in protein expression were revealed by comparisons between spectra originated from fruit juice sac cells at different stages: (i) stage II versus early stage II and (ii) stage III versus stage II. The complete data of the differential proteins detected can be found in Supplementary Tables S1 and S2 at *JXB* online. The analysis revealed a significant metabolic change occurring during the transition from early stage II to stage II and from stage II to stage III (see Supplementary Fig. S1 at *JXB* online). Although these changes involved a wide range of processes, this study focuses on protein changes related to primary metabolism.

Processes involving sugar metabolism, the TCA cycle, amino acid metabolism, energy production, and cell wall-related metabolism changed significantly in citrus juice sac cells during fruit development. Citrus fruit accumulate large amounts of sugars, mainly sucrose, glucose, and fructose. Enzymes participating in sucrose metabolism were highly represented in the proteome analysis of citrus fruit juice sac cells. Most of the enzymes involved in sucrose degradation and glycolytic pathways were up-regulated during the transition from early stage II to stage II and were up-regulated toward maturation, emphasizing the regulatory role of glycolysis in sugar utilization to drive fruit growth during citrus fruit development (Table 1; Fig. 1). Hexokinase, fructokinase, glucose-6-phosphate isomerase, fructose-*bis*phosphate aldolase, ATP-dependent 6-phosphofructose-1-kinase, triosephosphate isomerase, and enolase protein expression did not change significantly during the early stages and were up-regulated during the transition from stage II to stage III. UDP-glucose pyrophosphorylase, phosphoglucomutase, glyceraldehyde-3-phosphate dehydrogenase, 2,3-biphosphoglycerate-independent phosphoglycerate mutase, phosphoglycerate kinase, phosphoenolpyruvate carboxylase, and phosphoenolpyruvate carboxykinase were up-regulated throughout fruit development. Two pyruvate kinases were identified: iCitrus ID 52671 that did not change during the transition from early stage II to stage II and iCitrus ID 28935 that was up-regulated at stage II compared witho early stage II. Both proteins were up-regulated during the transition from stage II to stage III. Sucrose synthase was found to be an interesting exception, since it was down-regulated during the transition from early stage II to stage II, and was up-regulated nearer to maturation (Fig. 1; Table 1; see Supplementary Fig. S1 at *JXB* online). Four citrus sucrose synthase isoforms derived from four different unigenes were identified and clustered into three groups according to their sequence homology. Group 1 consisted of isoforms with homology to unigenes related to CitSUSA (Komatsu *et al.*, 2002), group 2 consisted of proteins derived from unigenes related to CitSUS1 (Komatsu *et al.*, 2002), and group 3 comprised CitSUS4, shown in this study to be expressed in the fruit. The expression patterns of CitSUS1 and CitSUSA were in agreement with their corresponding transcripts and with previously characterized enzymatic activities (Komatsu *et al.*, 2002; Katz *et al.*, 2007). The *CitSUS1* gene was shown to be expressed in the early stages of fruit development and its expression decreased towards maturation, while the *CitSUSA* gene was up-regulated towards maturation.

Table 1. Glycolysis and sugar metabolism related proteins identified by dMS and SC after search of the iCitrus database using X!Tandem with LC-MS/MS spectra

Annotation		iCitrus ID	Blast Hit to TAIR	Stage II versus early stage II					Stage III versus stage II				
				dMS No. peptides	Ratio	Direction	SC Bayes factor	Fold change	dMS No. peptides	Ratio	Direction	SC Bayes factor	Fold change
Sucrose synthase	CitSUSA	33122	At4g02280	–	–	–	–	–	3	27.33	–	–	–
	CitSUS4	18627	At5g20830	2	0.02	–	–	–	–	–	–	–	–
	CitSUS1	25199	At3g43190	2	0.03	–	–	–	–	–	–	–	–
		33038	At1g73370	8	0.01	–1	34022.5	37.08	3	6.86	1	57.57	6.96
Hexokinase		30768	At2g19860	5	1.39	0	2.70	2.41	3	148.9	0	0.70	1.11
Fructokinase		62294	At5g51830	–	–	0	1.00	1.00	–	–	1	221.90	13.69
		29116	At3g59480	–	–	0	4.91	6.50	3	3.93	0	0.67	1.21
Sucrose phosphate synthase		62092	At1g04920	–	–	1	10.79	10.53	–	–	0	8.47	3.45
UDP-glucose pyrophosphorylase		10418	At3g03250	4	19.6	–	–	–	10	111.2	1	13129	32.79
		18602	At5g17310	2	6.05	–	–	–	4	4.13	–	–	–
Phosphoglucomutase		60519	At1g23190	7	37.1	0	6.65	3.87	6	5.68	0	6.53	2.32
Glucose-6-phosphate isomerase		21361	At5g42740	–	–	0	1.00	1.00	–	–	1	72.50	10.41
PPi-dependent 6-phosphofructose-1-kinase;	CitPFP1	28806	At1g12000	–	–	0	1.00	1.00	–	–	–1	54.30	6.23
	CitPFP2	61196	At1g20950	–	–	0	1.25	3.23	3	9.55	0	1.29	1.62
ATP dependent 6-phosphofructose-1-pinase; PFK1		35527	At4g26270	–	–	0	1.00	1.00	–	–	1	19.61	4.69
Fructose-*bis*phosphate aldolase		22988	At2g36460	9	0.61	0	0.63	1.41	16	45.05	0	0.30	1.31
		246	At2g01140	5	0.67	–1	257.71	21.93	9	5.80	0	0.71	1.16
		21203	At2g01140	–	–	–	–	–	4	3.16	0	0.97	1.34
Triosephosphate isomerase		43479	At3g55440	5	0.77	0	1.47	1.69	5	3.20	0	0.77	1.32
		31271	At3g55440	3	0.58	0	1.65	3.93	4	4.57	0	1.05	1.48
Glyceraldehyde-3-phosphate dehydrogenase		37538	At3g04120	4	16.4	0	0.44	1.75	5	15.33	0	0.75	1.65
		948	At3g04120	5	10.1	-	–	–	5	7.24	–	–	–
		24071	At1g13440	7	9.10	1	21.98	3.00	7	57.00	0	1.56	1.20
Phosphoglycerate kinase		58537	At1g56190	7	42.0	1	6593.8	6.65	13	9.52	0	0.40	1.08
		4747	At1g79550	2	36.0	–	–	–	5	5.60	–	–	–
2,3-biphosphoglycerate-independent		40745	At1g09780	2	3.10	0	1.00	1.00	8	6.46	1	16.61	3.44
Phosphoglycerate mutase		28138	At3g08590	–	–	0	0.98	1.03	–	–	0	0.71	1.18
Enolase		61481	At2g36530	11	0.90	0	1.72	1.25	19	6	0	0.53	1.08
		832	At2g36530	4	0.99	–	–	–	6	3.10	–	–	–

Table 1. *Continued*

Annotation	iCitrus ID	Blast Hit to TAIR	Stage II versus early stage II					Stage III versus stage II				
			dMS No. peptides	Ratio	Direction	SC Bayes factor	Fold change	dMS No. peptides	Ratio	Direction	SC Bayes factor	Fold change
	15421	At2g36530	4	0.73	–	–	–	4	4.54	–	–	–
Pyruvate kinase	52671	At2g36580	2	1.42	0	0.62	1.17	3	2.15	0	0.60	1.13
	37060	At2g36580	–	–	–	–	–	3	2.20	–	–	–
	28935	At5g08570	4	12.3	0	0.41	1.27	5	2.84	0	1.16	1.82
Phosphoenolpyruvate carboxylase	60990	At1g53310	7	2.26	0	0.26	1.42	3	2.54	0	3.33	2.29
Phosphoenolpyruvate	51484	At5g65690	2	3.10	1	19.13	3.03	11	7.34	0	1.22	1.49
Carboxykinase invertase/pectin methylesterase inhibitor	30454	At3g17130	3	1.12	0	0.689	1.39	3	30.8	1	24.05	9.35

Proteins identified by dMS were considered to be up-regulated when expression fold change >2, not changed when fold change >0.5 but <2, and down-regulated when fold change was <0.5. For SC, a Bayes factor of >10 was considered significantly different. The column 'Direction' under SC represents up-regulated=1, no change=0, down-regulated= −1.

In this study, it is shown that the amounts of both CitSUS1 isoforms decreased in the transition from early stage II to stage II while that of iCitrus ID 33038 increased during the transition from stage II to stage III (Table 1) similar to CitSUSA which was up-regulated towards maturation, in agreement with the gene expression profiles and enzyme activity (Komatsu *et al.*, 2002). In addition, CitSUS4 was found to be significantly down-regulated between early stage II and stage II and was not detected in the later stage of fruit development (Table 1), thus indicating that its amounts remained constant.

The reaction mediated by phosphofructokinase (PFK) is one of the key control points of glycolysis in plants (Mustroph *et al.*, 2007). This reaction catalyses the interconversion of fructose-6-phosphate and fructose-1,6-*bis*phosphate. While most glycolytic enzymes are highly conserved between organisms, two types of phosphofructokinase isoforms exist in plants (Mustroph *et al.*, 2007). In addition to the ATP-dependent phosphofructokinase (PFK), a pyrophosphate-fructose-6-phosphate-phosphotransferase (PFP) uses pyrophosphate as the phosphoryl donor. Phosphorylation of fructose-6-phosphate catalysed by PFK is virtually irreversible while PFP catalyses the reaction in both directions. In citrus juice cells, two PFPs and one PFK were found to be differentially expressed (Table 1). CitPFP1 and CitPFP2 remained unchanged during the transition from early stage II to stage II. CitPFP1 was down-regulated during the transition from stage II to stage III while CitPFP2 was up-regulated. Gene expression analysis of *CitPFP1* and *CitPFP2* showed similar expression patterns (Fig. 1c). In contrast to PFPs, only one PFK was identified (CitPFK1) and its expression did not change during the transition from early stage II to stage II but was up-regulated during the transition from stage II to stage III.

No changes in invertases, an important family of proteins responsible for sucrose degradation to glucose and fructose, were seen in our proteomics analysis. The activity of two citrus acid invertases were detected in juice sac cells (Kubo *et al.*, 2001) with higher activities at the earlier stages of development. Since no differences in invertase proteins were detected in our comparisons, the expression of three citrus invertase genes, the vacuolar/acidic *βFruct1* and *βFruct2* and the neutral/alkaline invertase *CitCINV1*, was followed. The expression of these three genes peaked at early stage II and was down-regulated during the later stages of fruit development, suggesting a role of invertases during the early stages of fruit development (Fig. 1c). Interestingly, an invertase inhibitor protein (iCitrus ID 30454) was found between early stage II and stage II, and was up-regulated during the transition from stage II to stage III (detected in both dMS and SC). Invertase inhibitors are responsible for the decrease in invertase activity and function at the later stages of fruit development, highlighting the importance of sucrose synthase activity in sucrose degradation during these developmental stages.

Sucrose-phosphate synthase (SPS), an enzyme involved in sucrose synthesis, was up-regulated during the transition from early stage II to stage II and remained unchanged during the transition from stage II to stage III, while no changes were seen in sucrose-6-phosphate phosphatase

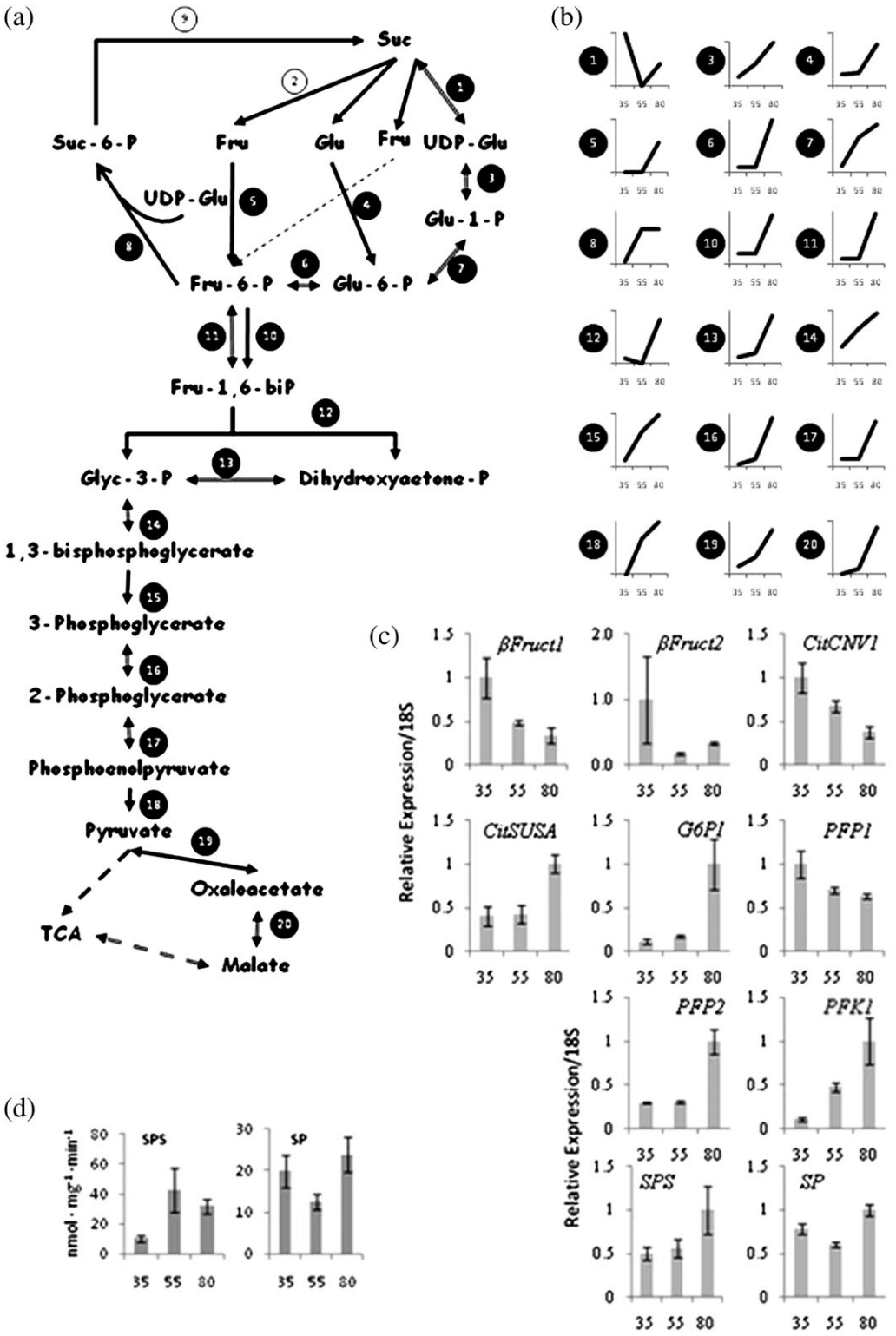

Fig. 1. Changes in glycolysis and sucrose metabolism during citrus fruit development. (a) Glycolysis and sucrose biosynthesis pathway. Enzymes that were found to be differentially expressed are numbered with a black background. Enzymes that remain unchanged are numbered with a white background. (1) Sucrose synthase. (2) Invertase. (3) UDP-Glu-pyrophosphorylase. (4) Hexokinase. (5) Fructokinase. (6) Glucose-6-P-isomerase. (7) Phosphoglucomutase. (8) Sucrose-phosphate-synthase. (9) Sucrose-phosphatase. (10) ATP-dependent phosphofructokinase. (11) PPi-dependent phosphofructokinase. (12) Fructose-*bis*phosphate aldolase. (13) Triose-phosphate-isomerase. (14) Glyceraldehyde-3-phosphate dehydrogenase. (15) Phosphoglycerate kinase. (16) Phosphoglycerate mutase. (17) Enolase. (18) Pyruvate kinase. (19) PEP carboxylase. (20) Malate dehydrogenase. (b) Protein expression changes of the above proteins during the transition from early stage II to stage II and from stage II to stage III. The figure shows enzyme changes as a function of development. The *x*-axis represents the three stages sampled: 35, early stage II; 55, stage II; 80, stage III. The *y*-axis represents the

(SPP), which mediates the formation of sucrose from sucrose-6-P. Some differences between SPS and SPP protein amounts and their levels of gene expression were noted. The expression of *SPS* was up-regulated only during the transition from stage II to stage III (Fig. 1c). Also, although no differences were seen in SPP protein amounts, the gene expression decreased slightly towards stage II and increased towards stage III (Fig. 1c). SPS and SPP activities correlated well with their protein expression patterns (Fig. 4d).

Changes in proteins involved in the TCA cycle during fruit development

Citrus fruits accumulate large amount of organic acids, mainly citrate, in juice sac cells. In contrast to sugars, citrate is synthesized in the juice cells and not transported from other organs of the tree. Citrate is produced through the TCA cycle and accumulates in the vacuole during fruit development, reaching a maximum at late stage II and decreasing towards maturation (Shimada *et al.*, 2006). Citrate is not only an intermediate metabolite in energy production in citrus juice cells, but also accumulates to high concentrations and is stored in the vacuole, contributing more than 90% of citrus fruit juice cells' organic acids content (Canel *et al.*, 1996; Spiegel-Roy and Goldschmidt, 1996). The mechanisms regulating citrate accumulation and degradation during pre- and post-harvest are unknown but play significant roles in determining the quality of many fruit species in general, and citrus fruit in particular. The pyruvate dehydrogenase enzyme complex links the TCA cycle to glycolysis. One of the pyruvate dehydrogenase complex (E1) proteins increased during the transition from early stage II to stage II while three others were down-regulated (Table 2). In addition, two other components of the pyruvate dehydrogenase complex, dihydrolipoamide *S*-acetyltransferase (E2) and dihydrolipoamide dehydrogenase (E3) were down-regulated during this transition. The pyruvate dehydrogenase complex (E1) was up-regulated during the transition from stage II to stage III (Fig. 2b; Table 2). Aconitase, isocitrate dehydrogenase, α-ketoglutarate dehydrogenase, succinyl-CoA synthetase, fumarase, and malate dehydrogenase were up-regulated or remained unchanged during the transition from early stage II to stage II, and were up-regulated during the transition from stage II to stage III (Fig. 2b; Table 2). Three exceptions to these general trends in the TCA cycle protein expression were noted, pyruvate dehydrogenase, succinate dehydrogenase, and malic enzyme, which were down-regulated during the transition from early stage II to stage II and were up-regulated during the transition from stage II to stage III.

Changes in organic acids, sugars, and sugar alcohols during fruit development

After determining protein changes in juice cells during fruit development, our focus turned to changes in core metabolite accumulation. The amounts of organic acids changed dramatically during fruit development. Organic acids of the TCA cycle, citrate, isocitrate, aconitate, and malate, were highest at stage II and decreased towards stage III, while 2-oxoglutarate and fumarate gradually decreased during fruit development and succinate accumulated mainly during stage III (Fig. 2c).

Sucrose, glucose, fructose, maltose, and sedoheptulose accumulated in an essentially linear manner during fruit development (Fig. 3). Galactose and trehalose rapidly accumulated in the juice sac cells towards maturation. Mannose gradually decreased during fruit development. Sugar alcohols displayed different accumulation patterns; inositol reached a maximum at stage II and decreased towards stage III, sorbitol decreased towards stage II and accumulated again towards maturation, while *myo*-inositol reached a maximum at the early stages of development and decreased gradually towards fruit maturation. Mannitol displayed considerable variation during development, increasing at stage II and decreasing towards maturation. Sugar phosphates and gluconate were higher at the earlier stages of fruit development and decreased during fruit maturation.

Changes in amino acid accumulation and proteins involved amino acid metabolism during fruit development

Plants assimilate inorganic nitrogen into four major amino acids, glutamate, glutamine, aspartate, and asparagine. These amino acids are usually transported from source to sink tissues and are used as a nitrogen source for metabolism and growth. The carbon skeletons for amino acids are derived from 3-phosphoglycerate, phosphoenolpyruvate or pyruvate generated during glycolysis or from 2-oxoglutarate and oxaloacetate generated in the citric acid cycle. The amounts of amino acids were highly variable during fruit development (Fig. 4). A gradual decline was noted for isoleucine and glutamine while a gradual increase was noted for shikimic acid, histidine, and tyrosine. Aspartate, asparagine, threonine, alanine, valine, leucine, glycine, serine, glutamate, and α-aminobutyrate peaked at stage II and decreased towards

calculated fold change ratio where stage II was assigned the value 1 and the values in early stage II and stage III were calculated according to the fold change found by dMS. An average of the different isoforms was calculated in cases where different protein isoforms were found (see also Table 1). (c) Changes in patterns of gene expression of invertases (β*Fruct1*, β*Fruct2*, *CitCNV1*), sucrose synthase (*CitSUSA*), glucose-6-P-isomerase (*G6PI*), PPi-dependent phosphofructokinase 1 and 2 (*PFP1* and *PFP2*), ATP-dependent phosphofructokinase (*PFK1*), sucrose-phosphate-synthase (*SPS*), and sucrose-phosphate phosphatase (*SPP*) during fruit development. The *x*-axis represents the three developmental stages as described in (b). (d) Sucrose-phosphate-synthase (SPS) and Sucrose-phosphate phosphatase (SPP) activities in juice sacs extract during fruit development.

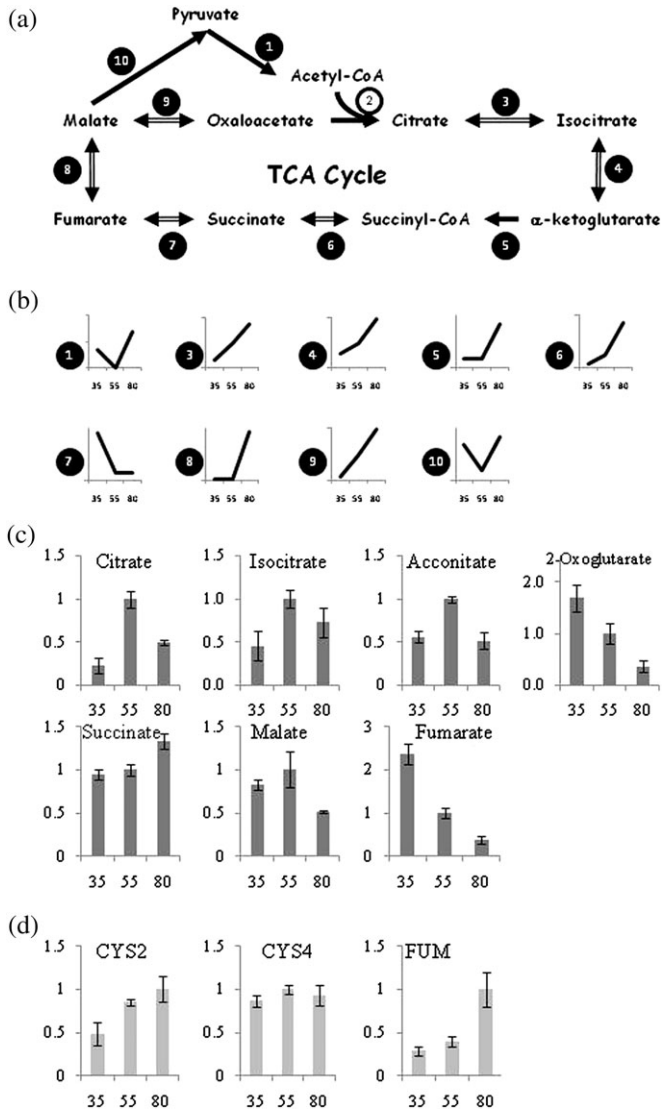

Fig. 2. Changes in the TCA cycle during citrus fruit development. (a) TCA cycle. Enzymes that were found to be differentially expressed are numbered with a black background. Enzymes that remained unchanged are numbered with a white background. (1) Pyruvate dehydrogenase. (2) Citrate synthase. (3) Aconitase. (4) Isocitrate dehydrogenase. (5) α-Ketoglutarate dehydrogenase/2-oxoglutarate dehydrogenase. (6) Succinyl-CoA synthetase. (7) Succinate dehydrogenase. (8) Fumerase. (9) Malate dehydrogenase. (10) Malic enzyme. (b) Protein expression changes of the above-mentioned proteins during the transition from early stage II to stage II and from stage II to stage III. The figure shows enzyme changes as a function of development. The *x*-axis represents the three stages sampled: 35, early stage II; 55, stage II; 80, stage III. The *y*-axis represents the calculated fold change ratio where stage II was assigned the value 1 and the values in early stage II and stage III were calculated according to the fold change found by dMS. An average of the different isoforms was calculated in cases where different protein isoforms were found (see also Table 1). (c) Relative content of TCA cycle intermediate accumulation was determined during citrus fruit development. Metabolite concentrations were normalized according to the concentration of each metabolite at stage II. (d) Quantitative PCR analysis for citrate synthase genes *CYS2, CYS4*, and fumarase *FUM*. The *x*-axis represents the three developmental stages as described in (b).

maturity. Homoserine, proline, arginine, and ornithine decreased towards late stage II and increased again towards maturity. Methionine and tryptophan showed a decrease only towards maturation and phenylalanine, β-alanine, lysine, and GABA (γ-aminobutyric acid) did not change during fruit development (Fig. 4).

Two aspartate aminotransferases were up-regulated during the transition from early stage II to stage II and from stage II to stage III and one was up-regulated during the transition from stage II to stage III (Table 3). In addition, two glutamine synthetases (iCitrus IDs 25117 and 678), catalysing the reaction synthesis of glutamine from glutamate, were up-regulated during the transition from early stage II to stage II, while two other isoforms (iCitrus IDs 2123 and 41697) remained stable. During the transition from stage II to stage III , iCitrus 41697 was up-regulated, iCitrus 2123 and iCitrus 678 remained unchanged, and iCitrus 25117 was down-regulated (Table 3). Another player in the amino acid core biosynthetic pathway is glutamate dehydrogenase (GDH) catalysing the reversible conversion of 2-oxoglutarate to glutamate. Two GDH proteins were identified; GDH3 was down-regulated during the transition from early stage II to stage II and was up-regulated during the transition from stage II to stage III and GDH2 was up-regulated during the transition from stage II to stage III (Table 3). The GABA shunt is suggested to be essential for plant growth (Bouché *et al.*, 2003) and to be pivotal in regulating citric acid degradation and fruit acidity during the later stage of citrus fruit development (Cercos *et al.*, 2006). Although significant changes in GABA were not detected, the three components of the GABA shunt [i.e. glutamate decarboxylase (GAD), GABA transaminase, and succinic semialdehyde dehydrogenase (SSADH)] displayed changes during fruit development. These enzymes, catalysing the decarboxylation of glutamate to GABA and CO_2, were up-regulated during the transition from early stage II to stage II and from stage II to stage III (Table 3). The level of GABA transaminase, catalysing the conversion of GABA to succinate semialdehyde, increased towards stage III. SSADH, mediating the oxidation of succinate semialdehyde to succinate, accumulated during the transition from early stage II to stage II and remained unchanged during the transition from stage II to stage III (Table 3).

Pyruvate supplies the carbon skeleton for alanine, leucine, and valine. Alanine aminotransferase and alanine:glyoxylate aminotransferase, both mediating alanine synthesis, remained unchanged at the early stages and were up-regulated during the late stage of development (Table 3). In the aspartate-derived amino acid biosynthesis pathway changes were identified in *S*-adenosyl-L-homocysteine hydrolases, methionine synthase, and ketol-acid reductiosomerase. *S*-adenosyl-L-homocysteine hydrolase and methionine synthase, active in the SAM cycle, were both down-regulated during the

Table 2. TCA cycle-related proteins identified by dMS and SC after search of the iCitrus database by X!Tandem using LC-MS/MS spectra

Annotation	iCitrus ID	Blast hit to TAIR	Stage II versus early stage II					Stage III versus stage II				
			dMS No. peptides	Ratio	Direction	SC Bayes factor	Fold change	dMS No.peptides	Ratio	Direction	SC Bayes factor	Fold change
Pyruvate dehydrogenase complex E1	22606	At1g24180	4	9.90	0	1.87	2.14	–	–	0	0.69	1.08
	1564	At1g24180	2	0.01	–	–	–	–	–	–	–	–
	23699	At5g50850	6	0.20	–1	21.69	8.81	3	24.16	0	3.64	2.84
	17446	At5g50850	2	0.22	–	–	–	–	–	–	–	–
Dihydrolipoamide *S*-acetyltransferase E2	42695	At3g17240	2	0.11	–	–	–	–	–	–	–	–
Dihydrolipoamide dehydrogenase E3	4911	At1g48030	4	0.26	–	–	–	–	–	–	–	–
	44669	At1g48030	7	0.33	–1	142.43	10.83	3	4.74	0	0.71	1.13
Aconitase	43680	At2g05710	2	25.29	0	1.00	1.00	2	13.64	1	143.42	12.24
	45840	At2g05710	4	49.72	0	0.40	1.08	4	4.77	0	0.58	1.29
	39802	At2g05710	3	24.94	0	0.66	1.88	4	33.48	1	30.46	5.52
Isocitrate dehydrogenase ($NADP^+$)	30767	At1g54340	2	2.15	0	4.329	7.19	7	8.92	0	0.744	1.03
	2385	At1g65930	–	–	–	–	–	2	8.40	–	–	–
	3923	At1g65930	–	–	–	–	–	3	4.43	–	–	–
	24612	At3g09810	2	1.31	0	1.16	2.03	2	0.80	0	1.57	1.95
	149	At4g35260	3	0.53	0	4.43	2.77	–	–	0	0.80	1.28
2-oxoglutarate dehydrogenase E1	53498	At3g55410	–	–	0	1.76	3.59	2	335.26	1	22.20	4.96
	1249	At3g55410	–	–	0	1.52	2.86	2	39.54	0	0.70	1.22
	38819	At3g55410	–	–	0	0.98	1.03	2	136.04	1	22.11	4.73
succinyl-CoA ligase	26895	At2g20420	3	5.29	1	104.00	17.39	4	298.60	0	0.65	1.05
	5556	At2g20420	–	–	–	–	–	3	327	–	–	–
	22272	At5g08300	2	0.95	0	0.62	1.23	2	3.41	0	1.19	1.53
Succinate dehydrogenase	61503	At2g18450	4	0.20	0	0.54	1.27	x	x	0	0.78	1.20
	55144	At5g40650	–	–	–1	14.30	6.42	–	–	0	9.83	3.68
	1184	At5g66760	2	0.24	–	–	–	–	–	–	–	–
Fumarase	23918	At2g47510	–	–	0	1.57	3.97	4	23.59	1	26.92	5.03
	920	At2g47510	–	–	–	–	–	2	6.64	–	–	–
Malate dehydrogenase	2641	At1g04410	2	11.92	–	–	–	6	4.65	–	–	–
	2305	At3g15020	3	0.49	0	1.63	2.90	2	2.55	0	0.87	1.64
	33986	At5g43330	3	6.84	1	12.60	3.68	9	9.00	1	41.23	4.25
NADP-malic enzyme	37162	At1g79750	7	0.48	0	0.70	1.08	11	2.57	0	0.23	1.35
	1735	At1g79750	4	0.45	–	–	–	6	2.57	–	–	–
	35283	At5g25880	2	0.42	–	–	–	2	4.86	–	–	–
	4879	At5g25880	2	0.42	–	–	–	–	–	–	–	–
	36024	At2g13560	2	0.10	0	2.47	5.78	–	–	0	1.00	1.00
	30233	At2g13560	2	0.26	–1	24.60	11.91	–	–	0	1.65	2.07

Proteins identified by dMS were considered to be up-regulated when expression fold change >2, not changed when fold change >0.5 but <2, and down-regulated when fold change was <0.5. For SC, a Bayes factor of >10 was considered significant difference. The column 'Direction' under SC represents up-regulated=1, no change=0, own-regulated= –1.

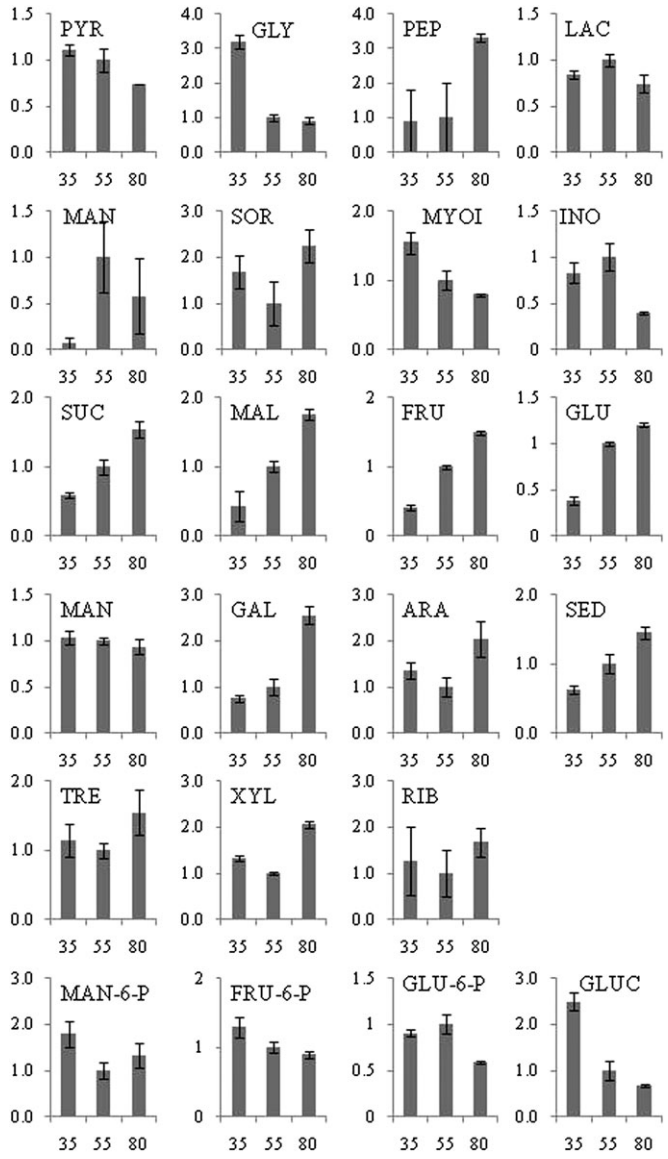

Fig. 3. Metabolic profiles of citrus juice sac cells during development. The relative content of glycolysis intermediates, sugars, sugar-phosphates, and sugar alcohols was determined during three stages of citrus fruit development, early stage II, stage II, and stage III. PYR, pyruvate; GLY, glycerate; PEP, phosphoenolpyruvate; LAC, lactate; MAN, mannitol; SOR, sorbitol; MYOI, *myo*-inositol; INO, inositol; SUC, sucrose; MAL, maltose; FRU, fructose; GLU, glucose; MAN, mannose; GAL, galactose; ARA, arabinose; SED, sedoheptulose; TRE, trehalose; XYL, xylose; RIB, ribose; MAN-6-P, mannose-6-phosphate; FRU-6-P, fructose-6-phosphate; GLU-6-P, glucose-6-phosphate; GLUC, gluconate. Metabolite concentrations were normalized according to the concentration of each metabolite at stage II. The *x*-axis represents the three developmental stages as described in Figs 1 and 2. The *y*-axis represents the relative contents of the different metabolites with respect to the metabolite content at Stage II (assigned the value of 1).

transition from early stage II to stage II and were up-regulated during the transition from stage II to stage III (Table 3).

Correlation in metabolite changes during fruit development

The use of two-way hierarchical clustering of metabolite amounts allowed the grouping of metabolites according to their accumulation trends (Fig. 5). Metabolites were separated into five different clusters: (i) pyruvate, mannose, methionine, tryptophan, leucine, 2-oxoglutarate, isoleucine, fumarate, glutamine, *myo*-inositol, fructose-6-P, glycerate, and gluconate were clustered together (Fig. 5) and their amounts declined during development and maturation (Figs. 2, 3, 4, 6). In two clusters: (ii) lactate, α-aminobutyrate, asparagine, γ-aminobutyrate, alanine, serine, valine, threonine, malate, inositol, and glucose-6-P; and (iii) citrate, 3-phosphoglycerate, glycine, aconitate, aspartate, and glutamate amounts increased from early stage II to stage II followed by a decline in their amounts in stage III. Two additional clusters of metabolites (iv) including β-alanine, tyrosine, phosphoenolpyruvate, xylose, lysine, sorbitol, arginine, and mannose-6-phosphate and (v) phenylalanine, ornithine, trehalose, arabinose, proline, ribose, succinate, shikimate, galactose, sedoheptulose, sucrose, isocitrate, mannitol, histidine, maltose, fructose, and glucose increased during both stage II and stage III. Interestingly, almost all sugars (except for mannose) displayed the same trend of accumulation towards fruit maturation.

Discussion

Metabolic shift during citrus fruit development

In this study, differential quantitative proteomics and metabolite profiling were used to assess developmental changes of citrus fruits. Most of the organic acids and many of the amino acids branching out from glycolysis and the TCA cycle peaked at stage II and declined during stage III of development. On the other hand, most of the sugars increased during stage III. No correlation was found between citrate accumulation and the expression of enzymes participating in citrate biosynthesis and degradation. Interestingly, citrate synthase protein amounts remained constant while aconitase, mediating the first step of citrate catabolism, isomerizing citrate to isocitrate, was up-regulated during fruit development.

The TCA cycle maintains a cyclic flux in order to generate reducing NADH and $FADH_2$ facilitating ATP synthesis by oxidative phosphorylation. Beyond the maintenance of a cyclic flux, the TCA cycle also functions to provide carbon skeletons for biosynthetic pathways as well as to metabolize organic acids generated from other pathways (Sweetlove *et al.*, 2010). The reduced expression of some of the proteins involved in the TCA cycle during the transition from early stage II to stage II such as pyruvate dehydrogenase, succinate dehydrogenase, and malic enzyme suggest a non-cyclic flux controlled by the influx of citrate and malate from the vacuole into the cytosol for its use in the TCA cycle. The changes in metabolite amounts throughout fruit development, with little correlation with protein expression levels, would also suggest that a large

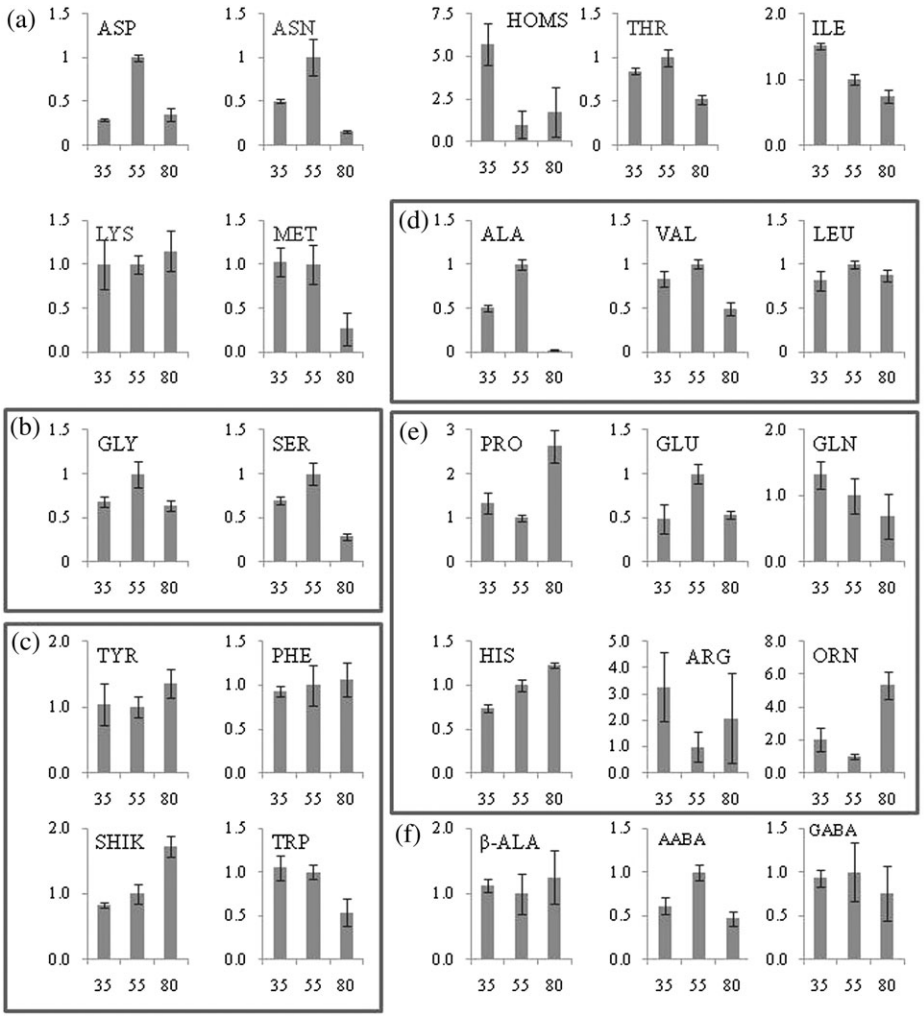

Fig. 4. Amino acid and metabolite profiles of citrus juice sac cells during development. The relative content of primary metabolites was determined during three stages of citrus fruit development, early stage II, stage II, and stage III. Amino acids derived from (a) oxaloacetate, (b) 3-phosphoglycerate, (c) phosphoenolpyruvate, (d) pyruvate, and (e) 2-oxoglutarate are clustered in separate boxes. ASP, aspartate; ASN, asparagine; HOMS, homoserine, THR, threonine; ILE, isoleucine; LYS, lysine; MET, methionine; ALA, alanine; VAL, valine; LEU, leucine; GLY, glycine; SER, serine; PRO, proline; GLU, glutamate; GLN, glutamine; TYR, tyrosine; PHE, phenylalanine; HIS, histidine; ARG, arginine; ORN, ornithine; SHIK, shikimic acid; TRP, tryptophan; β-ALA, β-alanine; AABA, α-aminobutyrate; GABA, γ- aminobutyrate. The *x*-axis represents the three developmental stages as described in Figs 1 and 2. The *y*-axis represents the relative contents of the different metabolites with respect to the metabolite content at stage II (assigned the value of 1).

proportion of metabolism regulation occurs at the post-translational level (Gibon *et al.*, 2004; Usadel *et al.*, 2005; Carrari *et al.*, 2006; Kummel *et al.*, 2006). The increase in glutamate dehydrogenase, glutamate decarboxylase, and γ-aminobutyrate transaminase protein expression and the patterns of GABA and succinate accumulation indicates that the GABA shunt is active.

In citrus, sucrose is transported into the juice cells through the apoplast and accumulates mainly in the vacuole (Koch, 1984; Koch and Avigne, 1990). Sucrose is then degraded to glucose and fructose by invertases or to fructose and UDP-glucose by sucrose synthase (Lowell *et al.*, 1989). While invertases did not appear to change at the protein level, the expression of three known invertase genes decreased during fruit development (Fig. 1c). Early studies have shown that acidic invertase activities in both grapefruit and Satsuma mandarin were initially high and decreased to very low levels at fruit maturation (Lowell *et al.*, 1989). The role of invertases in plant development is well established and the cleavage of sucrose is of key importance in the generation of hexoses needed for metabolism and signalling (Vargas and Salerno, 2010). In addition to transcriptional control, invertase activity can be regulated post-translationally by the action of invertase inhibitors (Jin *et al.*, 2009). Interestingly, an invertase inhibitor was up-regulated towards maturation, suggesting its potential role in the previously described decrease in invertase activity in citrus fruits (Lowell *et al.*, 1989). As invertase inhibitor proteins have also been implicated in the regulation of sugar metabolism in grape and peach fruits (da Silva *et al.*, 2005; Ziliotto *et al.*, 2008), their role in the control of fruit quality warrants further

Table 3. Amino acid metabolism related proteins identified by dMS and SC after search of the iCitrus database using X!Tandem with LC-MS/MS uninterpreted spectra

Annotation	iCitrus ID	Blast hit to TAIR	Stage II versus early stage II					Stage III versus stage II				
			dMS No. peptides	Ratio	Direction	SC Bayes factor	Fold change	dMS No. peptides	Ratio	Direction	SC Bayes factor	Fold change
Acetyl-CoA C-acyltransferase	55738	at1g04710	–	–	0	1.25	3.23	–	–	1	11.30	7.63
BCAT-2; branched-chain-amino-acid transaminase	15175	at1g10070	–	–	0	0.98	1.03	–	–	0	3.69	2.90
Aminomethyltransferase	40906	at1g11860	–	–	0	0.98	1.03	2	13.50	0	1.51	1.81
Glycine dehydrogenase	56681	at2g26080	3	0.20	–1	452.08	20.99	–	–	0	0.99	1.24
ALAAT1 (alanine aminotransferase)	35404	at1g17290	–	–	0	1.00	1.00	–	–	1	587.23	15.56
PGDH (3-phosphoglycerate dehydrogenase)	33085	at1g17745	7	23.49	0	0.32	1.19	4	2.04	0	5.82	2.29
PGDH (3-phosphoglycerate dehydrogenase)	4033	at4g34200	3	0.73	–	–	–	2	2.26	–	–	–
AGT2 (alanine:glyoxylate aminotransferase 2)	12839	at4g39660	–	–	–	–	–	3	18.30	–	–	–
AGT2 (alanine:glyoxylate aminotransferase 2)	27165	at4g39660	–	–	0	0.98	1.03	4	16.42	0	1.69	1.93
ASP4 (aspartate aminotransferase 4)	40919	at1g62800	2	9.08	–	–	–	3	41.05	–	–	–
ASP4 (aspartate aminotransferase 4)	25228	at1g62800	2	9.08	1	64.43	7.15	4	38.73	1	14.81	3.34
ASP3 (aspartate aminotransferase 3)	14798	at5g11520	–	–	–	–	–	2	7.30	–	–	–
GAD2 (glutamate decarboxylase 2)	45590	at1g65960	2	1924.40	0	1.00	1.00	4	2.15	0	1.75	2.1
GAD2 (glutamate decarboxylase 2)	60356	at1g65960	2	239.09	1	696.64	26.44	5	2.06	0	0.49	1.06
GAD1 (glutamate decarboxylase 1)	58418	at3g17760	–	–	–	–	–	2	1.47	–	–	–
GDH3(glutamate dehydrogenase 3)	45569	at3g03910	–	–	-1	41.11	11.21	2	6.64	0	2.31	2.23
GDH2 (glutamate dehydrogenase 2)	37770	at5g07440	–	–	–	–	–	2	6.64	–	–	–
GLN1;3 (glutamine synthetase)	2123	at3g17820	–	–	0	1.00	1.00	–	–	0	7.38	6.85
GLN1;1-GSR1(glutamine synthetase)	25117	at5g37600	5	161.07	1	1197.34	4.24	6	0.67	–1	16.77	1.88
GLN1;1-GSR1(glutamine synthetase)	41697	at5g37600	–	–	0	1.00	1.00	–	–	1	92.46	12.23
GLN1;1-GSR1(glutamine synthetase)	678	at5g37600	2	180.37	–	–	–	–	–	–	–	–
?-Aminobutyrate transaminase	22281	at3g22200	–	–	–	–	–	3	13.87	–	–	–
P5CS1 (delta1-pyrroline-5-carboxylate synthase 1)	37246	at2g39800	3	0.32	–1	24.08	7.09	–	–	0	1.07	1.48
ALDH12A1, 1-pyrroline-5-carboxylate dehydrogenase	27988	at5g62530	2	0.17	0	7.46	8.52	–	–	0	1.00	1.00
MS2 (methionine synthase 2)	41927	at3g03780	5	0.14	–	–	–	4	1.16	–	–	–
MS2 (methionine synthase 2)	43263	at3g03780	11	0.16	–1	13256.47	31.34	11	5.38	0	0.51	1.60
MS1 (methionine synthase 1)	24003	at5g17920	–	–	–	–	–	3	16.69	–	–	–

Table 3. *Continued*

Annotation	iCitrus ID	Blast hit to TAIR	Stage II versus early stage II					Stage III versus stage II				
			dMS No. peptides	Ratio	Direction	SC Bayes factor	Fold change	dMS No. peptides	Ratio	Direction	SC Bayes factor	Fold change
SAHH2 (*S*-adenosyl-L-homocysteine hydrolase 2)	11482	at3g23810	–	–	–	–	–	2	1.73	–	–	–
SAHH2 (*S*-adenosyl-L-homocysteine hydrolase 2)	49170	at3g23810	9	0.17	–1	130.58	4.57	14	170.98	0	0.86	1.41
SAHH2 (*S*-adenosyl-L-homocysteine hydrolase 2)	51358	at3g23810	7	0.17	0	0.19	1.13	14	170.98	0	0.86	1.41
SAHH1 (*S*-adenosyl-L-homocysteine hydrolase 1)	1927	at4g13940	7	0.16	–	–	–	9	182.30	–	–	–
Ketol-acid reductoisomerase	22397	at3g58610	2	0.26	–1	23.24	10.72	–	–	–1	88.90	12.39
O-acetylserine(thiol)lyase	11065	at4g14880	2	14.31	1	33.25	12.26	–	–	0	9.65	3.28
Acetyl-CoA C-acyltransferase	33619	at5g47720	–	–	0	1.00	1.00	–	–	0	1.05	2.23
Succinate semialdehyde dehydrogenase	56374	at1g79440	2	2.3	0	1.27	1.74	–	–	0	0.75	1.07

Proteins identified by dMS were considered to be up-regulated when expression fold change >2, not changed when fold change >0.5 but <2, and down-regulated when fold change was <0.5. For SC, a Bayes factor of >10 was considered a significant difference. The column 'Direction' under SC represents up-regulated=1, no change=0, down-regulated= –1.

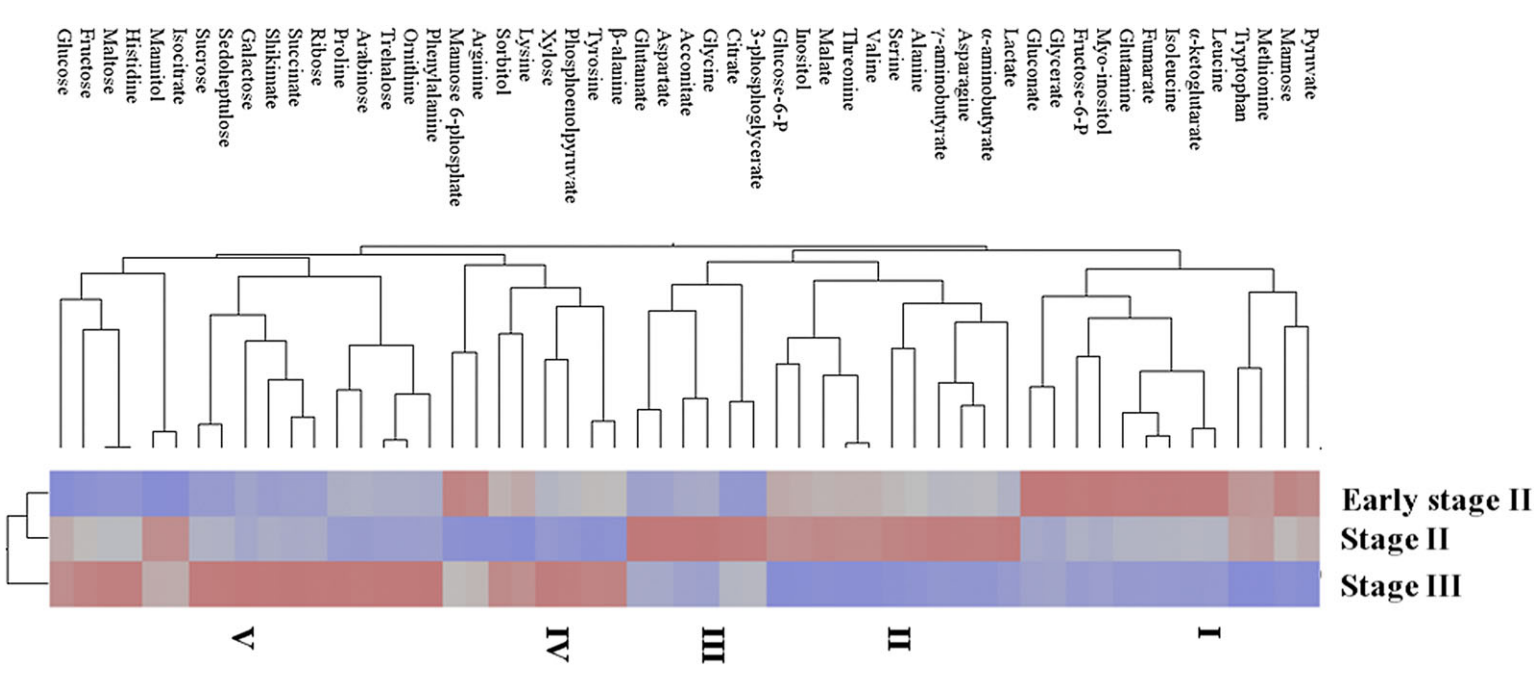

Fig. 5. Two-way hierarchical clustering of metabolites levels. Juice cells of citrus at early stage II, stage II, and stage III were collected. The red colour represents higher values and green represents lower relative values when compared with the mean metabolite value across all samples.

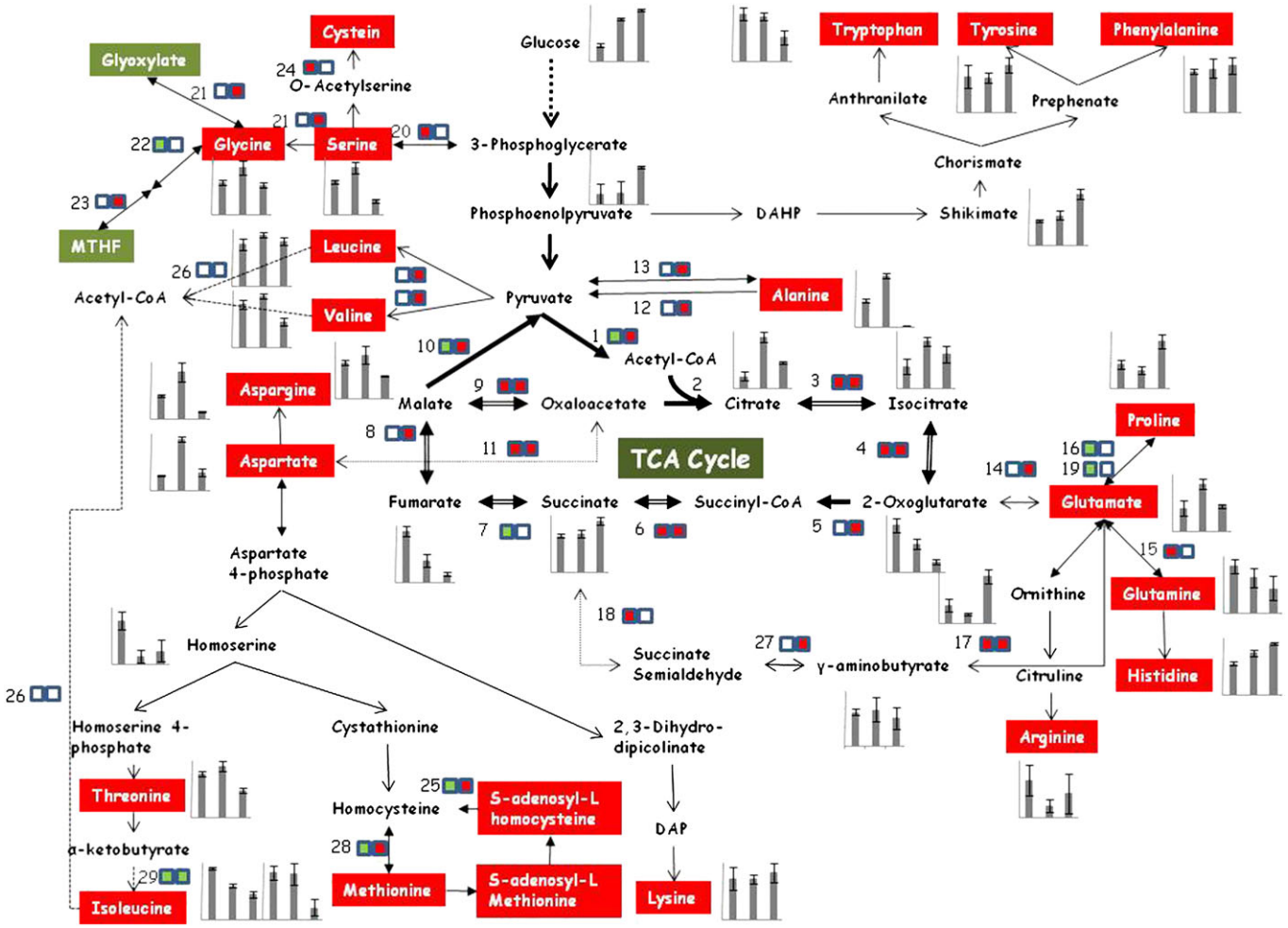

Fig. 6. Illustration of metabolism flow during citrus fruit development. Graphs represent the accumulation of organic and amino acids during early stage II, stage II, and stage III. Numbered boxes represent the protein expression trend; the left side represents the comparison of stage II versus early stage II and the right side represents the comparison of stage III versus stage II. Green represents down-regulation, white represents no change, and red represents up-regulation. (1) Pyruvate dehydrogenase. (2) Citrate synthase. (3) Aconitase. (4) Isocitrate dehydrogenase. (5) α-Ketoglutarate dehydrogenase/2-oxoglutarate dehydrogenase. (6) Succinyl-CoA synthetase. (7) Succinate dehydrogenase. (8) Fumarase. (9) Malate dehydrogenase. (10) Malic enzyme. (11) Aspartate aminotransferase. (12) Alanine:glyoxylate aminotransferase. (13) Alanine aminotransferase. (14) Glutamate dehydrogenase. (15) Glutamine synthetase. (16) 1-Pyrroline-5-carboxylate dehydrogenase. (17) Glutamate decarboxylase. (18) Succinate-semialdehyde dehydrogenase. (19) Delta1-pyrroline-5-carboxylate synthase 1. (20) PGDH (3-phosphoglycerate dehydrogenase). (21) Alanine:glyoxylate aminotransferase. (22) Glycine decarboxylase P-protein 2. (23) Aminomethyltransferase. (24) Cysteine synthase. (25) *S*-adenosyl-L-homocysteine hydrolase. (26) Branched-chain amino acid transaminase. (27) γ-Aminobutyrate transaminase. (28) Methionine synthase. (29) Ketol-acid reductoisomerase.

investigation. Sucrose synthase proteins decreased during the transition from early stage II to stage II and increased during the transition from stage II to stage III. This pattern correlated well with sucrose synthase enzymatic activity reported by Komatsu *et al.* (2002). Sucrose synthase can play important roles in sink strength and it was suggested that CitSUS1 may have a role in supplying UDP-glucose and fructose for cell wall synthesis during the cell division stage while CitSUSA and SUS1 may supply substrates for sucrose synthesis during maturation (Komatsu *et al.*, 2002). Two isozymes of sucrose synthase, each active during different stages of development (immature and mature), were also reported in pear (Suzuki *et al.*, 1996). Our results support the notion of a balance between the action of sucrose synthases and the regulation of invertase activities.

The accumulation of arabinose, galactose, xylose, and ribose, important for cell wall synthesis was correlated with proteins associated with cell wall metabolism such as cellulose synthase, pectin methylesterases, β-chitinase, PR4, β-1,3-glucanase, polygalacturonase inhibiting protein, and UDP-glucose 6-dhydrogenase.

The role of phosphoenolpyruvate (PEP) carboxylase in the metabolism of malate and citrate is intriguing. Pyruvate is generally the major product of glycolysis arising from PEP via the activity of pyruvate kinase. However, plant cells can

convert PEP to malate via oxaloacetate in reactions catalysed by PEP carboxylase (PEPC) and malate dehydrogenase (MDH). The resulting malate may be utilized as a respiratory substrate in the TCA cycle, or be converted to pyruvate via the activity of malic enzyme. As shown in potato tubers with reduced NAD-dependent malic enzyme activity, the conversion of malate to pyruvate can influence glycolytic flux (Jenner *et al.*, 2001; Sweetman *et al.*, 2009). Studies in tomato and grape fruits suggested the occurrence of gluconeogenesis in fruits, particularly during the ripening stage when sugars are accumulating rapidly. A correlation between citrate, malate, and oxaloacetate loss and the activities of PEPC and PEPCK (PEP carboxykinase) and gluconeogenesis in fruits was demonstrated (Sweetman *et al.*, 2009). Both of these proteins were up-regulated during citrus fruit development.

Our results suggest that organic acid and amino acid accumulation shifted toward sugar synthesis during the later stage of citrus fruit development. The notion of a metabolic shift during fruit maturation is supported by work on grape, strawberry, and tomato fruit maturation (Carrari *et al.*, 2006; Deluc *et al.*, 2007; Fait *et al.*, 2008). Gene expression analysis of maturing grapes showed that a decrease in expression of transcripts associated with organic acid accumulation was accompanied by the increased expression of genes associated with the TCA cycle and genes encoding enzymes mediating sugar accumulation (Deluc *et al.*, 2007). The observed increase in SPS and SPP activity in the later stages of fruit development, concomitant with the rapid accumulation of sucrose, suggest that this sugar is also being synthesized in citrus juice sac cells during fruit development and ripening.

Supplementary data

Supplementary data can be found at *JXB* online.

Supplementary Table S1. Protein expression data using spectral counting (dMS).

Supplementary Table S2. Protein expression data using spectral counting (SC).

Supplementary Table S3. List of primers used for qPCR analysis as described in the Materials and methods.

Supplementary Fig. S1. Visualization of metabolism overview using MapMan: (a) stage II versus early stage II, (b) stage III versus stage II.

Acknowledgements

This work was supported by a research grant No. US-4010-07C from BARD, the United States-Israel Binational Agricultural Research and Development Fund, and by the Will W Lester Endowment, University of California.

References

America AHP, Cordewener JHG. 2008. Comparative LC-MS: a landscape of peaks and valleys. *Proteomics* **8,** 731–749.

Bain JM. 1958. Morphological, anatomical, and physiological changes in the developing fruit of the Valencia orange, *Citrus sinensis* (L.) Osbeck. *Australian Journal of Botany* **6,** 1–23.

Bantscheff M, Schirle M, Sweetman G, Rick J, Kuster B. 2007. Quantitative mass spectrometry in proteomics: a critical review. *Analytical Biochemistry* **389,** 1017–1031.

Baxter CJ, Foyer CH, Turner J, Rolfe SA, Quick WP. 2003. Elevated sucrose-phosphate synthase activity in transgenic tobacco sustains photosynthesis in older leaves and alters development. *Journal of Experimental Botany* **54,** 1813–1820.

Bouché N, Fait A, Bouchez D, Møller SG, Fromm H. 2003. Mitochondrial succinic-semialdehyde dehydrogenase of the γ-aminobutyrate shunt is required to restrict levels of reactive oxygen intermediates in plants. *Proceedings of the National Academy of Sciences, USA* **100,** 6843–6848.

Bradford MM. 1976. A rapid and sensitive method for the quantitation of microgram quantities of proteins utilizing the principle of protein–dye binding. *Anaytical Biochemistry* **72,** 248–254.

Canel C, Bailey-Serres JN, Roose ML. 1996. Molecular characterization of the mitochondrial citrate synthase gene of an acidless pummelo (*Citrus maxima*). *Plant Molecular Biology* **31,** 143–147.

Carrari F, Baxter C, Usadel B, *et al*. 2006. Integrated analysis of metabolite and transcript levels reveals the metabolic shifts that underlie tomato fruit development and highlight regulatory aspects of metabolic network behavior. *Plant Physiology* **142,** 1380–1396.

Cercos M, Soler G, Iglesias DJ, Gadea J, Forment J, Talon M. 2006. Global analysis of gene expression during development and ripening of citrus fruit flesh. a proposed mechanism for citric acid utilization. *Plant Molecular Biology* **62,** 513–527.

Choi H, Fermin D, Nesvizhskii AI. 2008. Significance analysis of spectral count data in label-free shotgun proteomics. *Molecular and Cellular Proteomics* **7,** 2373–2385.

da Silva FG, Iandolino A, Al-Kayal F, *et al*. 2005. Characterizing the grape transcriptome. Analysis of expressed sequence tags from multiple *Vitis* species and development of a compendium of gene expression during berry development. *Plant Physiology* **139,** 574–597.

Deluc L, Grimplet J, Wheatley M, Tillett R, Quilici D, Osborne C, Schooley D, Schlauch K, Cushman J, Cramer G. 2007. Transcriptomic and metabolite analyses of Cabernet Sauvignon grape berry development. *BMC Genomics* **8,** 429.

Echeverria E. 1992. Activities of sucrose metabolising enzymes during sucrose accumulation in developing acid limes. *Plant Science* **85,** 125–129.

Echeverria E, Burns JK. 1990. Sucrose breakdown in relation to fruit growth of acid lime (*Citrus aurantifolia*). *Journal of Experimental Botnay* **41,** 705–708.

Elias JE, Haas W, Faherty BK, Gygi SP. 2005. Comparative evaluation of mass spectrometry platforms used in large-scale proteomics investigations. *Nature Methods* **2,** 667–675.

Fait A, Hanhineva K, Beleggia R, Dai N, Rogachev I, Nikiforova VJ, Fernie AR, Aharoni A. 2008. Reconfiguration of the achene and receptacle metabolic networks during strawberry fruit development. *Plant Physiology* **148,** 730–750.

Gibon Y, Blaesing OE, Hannemann J, Carillo P, Hohne M, Hendriks JHM, Palacios N, Cross J, Selbig J, Stitt M. 2004. A robot-based platform to measure multiple enzyme activities in

Arabidopsis using a set of cycling assays: comparison of changes of enzyme activities and transcript levels during diurnal cycles and in prolonged darkness. *The Plant Cell* **16,** 3304–3325.

Gibon Y, Usadel B, Blaesing O, Kamlage B, Hoehne M, Trethewey R, Stitt M. 2006. Integration of metabolite with transcript and enzyme activity profiling during diurnal cycles in Arabidopsis rosettes. *Genome Biology* **7,** R76.

Gygi SP, Rochon Y, Franza BR, Aebersold R. 1999. Correlation between protein and mRNA abundance in yeast. *Molecular and Cellular Biology* **19,** 1720–1730.

Harwood JE, van Steenderen RA, Kühn AL. 1969. A rapid method for orthophosphate analysis at high concentrations in water. *Water Research* **3,** 417–423.

Jenner HL, Winning BM, Millar AH, Tomlinson KL, Leaver CJ, Hill SA. 2001. NAD malic enzyme and the control of carbohydrate metabolism in potato tubers. *Plant Physiology* **126,** 1139–1149.

Jin Y, Ni DA, Ruan YL. 2009. Post-translational elevation of cell wall invertase activity by silencing its inhibitor in tomato delays leaf senescence and increases seed weight and fruit hexose level. *The Plant Cell* **21,** 2072–2089.

Kall L, Storey JD, MacCoss MJ, Noble WS. 2008. Assigning significance to peptides identified by tandem mass spectrometry using decoy databases. *Journal of Proteome Research* **7,** 29–34.

Katz E, Fon M, Eigenheer RA, Phinney BS, Sadka A, Blumwald E. 2010. A label-free differential quantitative mass spectrometry method for the characterization and identification of protein changes during citrus fruit development. *Proteome Science* **8,** 68.

Katz E, Fon M, Lee Y, Phinney B, Sadka A, Blumwald E. 2007. The citrus fruit proteome: insights into citrus fruit metabolism. *Planta* **226,** 989–1005.

Katz E, Lagunes PM, Riov J, Weiss D, Goldschmidt EE. 2004. Molecular and physiological evidence suggests the existence of a system II-like pathway of ethylene production in non-climacteric citrus fruit. *Planta* **219,** 243–252.

Keller A, Nesvizhskii AI, Kolker E, Aebersold R. 2002. Empirical statistical model to estimate the accuracy of peptide identifications made by MS/MS and database search. *Analytical Chemistry* **74,** 5383–5392.

Koch K. 2004. Sucrose metabolism: regulatory mechanisms and pivotal roles in sugar sensing and plant development. *Current Opinion in Plant Biology* **7,** 235–246.

Koch KE. 1984. The path of photosynthate translocation into citrus fruit. *Plant, Cell and Environment* **7,** 647–653.

Koch KE, Avigne WT. 1990. Post-phloem, non-vascular transfer in citrus: kinetics, metabolism, and sugar gradients. *Plant Physiology* **93,** 1405–1416.

Komatsu A, Moriguchi T, Koyama K, Omura M, Akihama T. 2002. Analysis of sucrose synthase genes in citrus suggests different roles and phylogenetic relationships. *Journal of Experimental Botany* **53,** 61–71.

Kubo T, Hohjo I, Hiratsuka S. 2001. Sucrose accumulation and its related enzyme activities in the juice sacs of satsuma mandarin fruit from trees with different crop loads. *Scientia Horticulturae* **91,** 215–225.

Kummel A, Panke S, Heinemann M. 2006. Putative regulatory sites unraveled by network-embedded thermodynamic analysis of metabolome data. *Molecular Systems Biology* **2,** 00342006.

Livak KJ, Schmittgen TD. 2001. Analysis of relative gene expression data using real-time quantitative PCR and the 2-[delta][delta]CT method. *Methods* **25,** 402–408.

Lowell CA, Tomlinson PT, Koch KE. 1989. Sucrose-metabolizing enzymes in transport tissues and adjacent sink structures in developing citrus fruit. *Plant Physiology* **90,** 1394–1402.

Lunn JE, Ashton AR, Hatch MD, Heldt HW. 2000. Purification, molecular cloning and sequence analysis of sucrose-6F -phosphate phosphohydrolase from plants. *Proceedings of the National Academy of Sciences, USA* **97,** 12914–12919.

Mounet F, Moing A, Garcia V, *et al*. 2009. Gene and metabolite regulatory network analysis of early developing fruit tissues highlights new candidate genes for the control of tomato fruit composition and development. *Plant Physiology* **149,** 1505–1528.

Mustroph A, Sonnewald U, Biemelt S. 2007. Characterisation of the ATP-dependent phosphofructokinase gene family from. *Arabidopsis thaliana. FEBS Letters* **581,** 2401–2410.

Nesvizhskii AI, Keller A, Kolker E, Aebersold R. 2003. A statistical model for identifying proteins by tandem mass spectrometry. *Analytical Chemistry* **75,** 4646–4658.

Roessner U, Wagner C, Kopka J, Trethewey RN, Willmitzer L. 2000. Simultaneous analysis of metabolites in potato tuber by gas chromatography-mass spectrometry. *The Plant Journal* **23,** 131–142.

Sadka A, Dahan E, Or E, Cohen L. 2000. NADP(+) isocitrate dehydrogenase gene expression and isozyme activity during citrus fruit development. *Plant Science* **158,** 173–181.

Schulze WX, Usadel B. 2010. Quantitation in mass-spectrometry-based proteomics. *Annual Review of Plant Biology* **61,** 491–516.

Shimada T, Nakano R, Shulaev V, Sadka A, Blumwald E. 2006. Vacuolar citrate/H^+ symporter of citrus juice cells. *Planta* **224,** 472–480.

Spiegel-Roy P, Goldschmidt EE. 1996. *Biology of citrus*. Cambridge University Press.

Suzuki A, Kanayama Y, Yamaki S. 1996. Occurrence of two sucrose synthase isozymes during maturation of Japanese pear fruit. *Journal of the American Society for Horticultural Science* **121,** 943–947.

Sweetlove LJ, Beard KFM, Nunes-Nesi A, Fernie AR, Ratcliffe RG. 2010. Not just a circle: flux modes in the plant TCA cycle. *Trends in Plant Science* **15,** 462–470.

Sweetman C, Deluc LG, Cramer GR, Ford CM, Soole KL. 2009. Regulation of malate metabolism in grape berry and other developing fruits. *Phytochemistry* **70,** 1329–1344.

Talon M, Gmitter FG. 2008. Citrus genomics. *International Journal of Plant Genomics doi:10.1155/2008/528361* .

Thimm O, Bläsing O, Gibon Y, Nagel A, Meyer S, Krüger P, Selbig J, Müller LA, Rhee SY, Stitt M. 2004. MapMan: a user-driven tool to display genomics data sets onto diagrams of metabolic pathways and other biological processes. *The Plant Journal* **37,** 914–939.

Tomlinson PT, Duke ER, Nolte KD, Koch KE. 1991. Sucrose synthase and invertase in isolated vascular bundles. *Plant Physiology* **97,** 1249–1252.

Usadel B, Nagel A, Thimm O, *et al*. 2005. Extension of the visualization tool MapMan to allow statistical analysis of arrays, display of coresponding genes, and comparison with known responses. *Plant Physiology* **138,** 1195–1204.

Vargas WA, Salerno GL. 2010. The Cinderella story of sucrose hydrolysis: alkaline/neutral invertases, from cyanobacteria to unforeseen roles in plant cytosol and organelles. *Plant Science* **178,** 1–8.

Ward JH. 1963. Hierarchical grouping to optimize an objective function. *Journal of the American Statistical Association* **58,** 236–244.

Wienkoop S, Morgenthal K, Wolschin F, Scholz M, Selbig J, Weckwerth W. 2008. Integration of metabolomic and proteomic phenotypes: analysis of data covariance dissects starch and RFO metabolism from low and high temperature compensation response in Arabidopsis thaliana. *Molecular Cell Proteomics* **7,** 1725–1736.

Zanor MI, Rambla J-L, Chaib J, Steppa A, Medina A, Granell A, Fernie AR, Causse M. 2009. Metabolic characterization of loci affecting sensory attributes in tomato allows an assessment of the influence of the levels of primary metabolites and volatile organic contents. *Journal of Experimental Botany* **60,** 2139–2154.

Ziliotto F, Begheldo M, Rasori A, Bonghi C, Tonutti P. 2008. Transcriptome profiling of ripening nectarine (*Prunus persica* L. Batsch) fruit treated with 1-MCP. *Journal of Experimental Botany* **59,** 2781–2791.